JMEPEG (2002) 11:631-639

Effect of Near-Surface Residual Stress and Microstructure Modification From Machining on the Fatigue Endurance of a Tool Steel

F. Ghanem, C. Braham, M.E. Fitzpatrick, and H. Sidhom

(Submitted 24 January 2002; in revised form 27 June 2002)

This study concerns the effect of machining on the fatigue life of an EN X155CrMoV12 tool steel (SAE J438b), with regard to the generation of near-surface residual stress and microstructural modification of the machined surface. Two possible methods for machining tool steels were compared: electro-discharge machining (EDM), a high energy density process, and milling, a more conventional cutting process. Particular attention was given to characterization of the surface roughness, microstructure, and residual stress, using a combination of microstructural analysis, crack observation, scanning electron microscopy (SEM), x-ray diffraction (XRD), and chemical composition changes by energy-dispersive x-ray. A decrease of around 35% in the fatigue limit was observed for the EDM samples, compared with the milled samples. This was attributed to a tensile residual stress state after EDM, combined with significant phase transformation and hydrogen embrittlement. The milled surfaces showed no microstructural transformation or surface cracking and contained compressive residual stresses, all of which contributed to an improved fatigue resistance.

Keywords electro-discharge machining, fatigue, surface integrity, tool steel

1. Introduction

The production of complex components, requiring fine surface details, in metal carbide tools or specialized mould steels, requires nonconventional machining techniques such as electron beam milling, laser milling, and electro-discharge machining (EDM).[1-3] During each electric discharge between the electrode tool and the workpiece, EDM involves a high energy density, which leads to extreme heating of the surface and can reach 3000-10 000 °C.[4] The temperature gradient created near the surface induces substantial modification of the thermally affected layers. These modifications depend on the nature of the material used in the workpiece and the heat source, controlled by conditions like the discharge intensity, its duration, and the type of dielectric used.[5-9] Many studies concerning the metallurgical transformations near the surfaces of material machined by EDM have been performed, without accounting for the generation of defects and residual stress by the process. These two factors have important consequences for the durability of materials used in conditions where surface wear and fatigue are important.[10,11] They are important in the premature deterioration of tool steels and molds fabricated using this process.[12-15] The few studies that have examined this problem are unanimous about the remarkable reduction in fatigue limit of EDM-machined pieces compared with those produced by classic processes like turning, drilling, grinding, and mechanical polishing, and also, to a lesser degree, by laser machining.[6,7,16-18] These studies, however, have not clearly established the role of surface integrity on in-service effects. In this context, we present results of a study of the influence of surface quality after EDM on the fatigue performance of a tool steel, type EN X155CrMoV12. Metallurgical transformations induced by the process and their consequence for surface integrity were determined with the aim of identifying their role on the bending fatigue limit. The results are compared with results from milled surfaces.

F. Ghanem and **H. Sidhom,** Laboratoire de Mécanique, Matériaux et Procédés, LABSTI03 ESSTT 5 Avenue Taha Husseïn B.P. 56, Bab Menara, 1008 Tunisia; **C. Braham,** Laboratoire de Microstructure et Mécanique des Matériaux, ENSAM, CNRS ESA 8006 151 bd de l'Hôpital, 75013 Paris, France; and **M.E. Fitzpatrick,** Dept of Materials Engineering, The Open University, Walton Hall, Milton Keynes MK7 6AA, United Kingdom. Contact e-mail: chedly.braham@paris.ensam.fr.

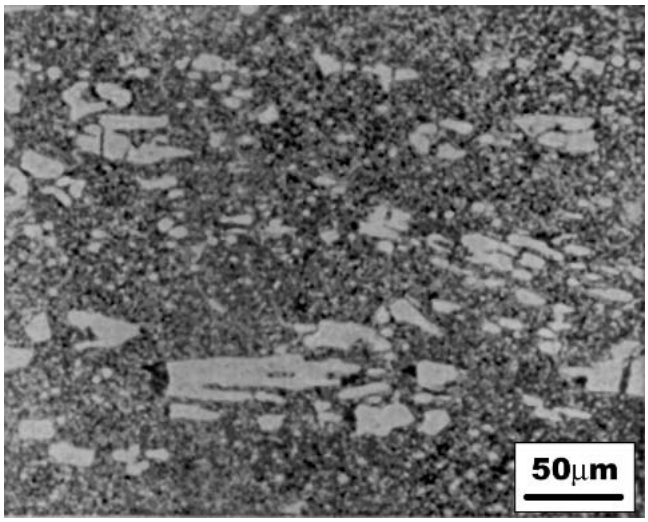

Fig. 1 Structure of as-received material, showing ferrite and carbides: the ferrite is the darker matrix, and the carbides are the lighter particles

2. Material and Machining Conditions

The material studied is a high-alloy steel, type EN X155CrMoV12 (SAE J438b). It is used in the fabrication of tools and molds, and EDM and milling techniques are therefore often applied to it. Its chemical composition and thermal properties are given in Tables 1 and 2. Its initial metallurgical state before machining is shown in Fig. 1, showing alloy carbides in a ferritic matrix after quenching and tempering of the material. The machining conditions used are shown in Tables 3 and 4 for the EDM and milling processes, respectively.

3. Experimental Methods

3.1 Surface Characterization

Three-dimensional roughness measurement equipment was used to characterize the surface topography. Two parameters were obtained: R_a (average roughness) and R_t (maximum roughness depth).

Metallurgical transformations, which occurred in the near-surface layers, were analyzed using optical metallographical observations carried out on a cross section of the sample.

The surface hardening from cold work was characterized by Vickers microhardness testing with a load of 100 gf.

Profiles of the residual stress in the sample were made near-surface using x-ray diffraction (XRD). XRD measurements were performed using a Set-X x-ray diffractometer (ELPHYSE, France), with the multiple psi (ψ) tilt method. The appropriate diffraction parameters are presented in Table 5. In-depth stress measurements were obtained using electrolytic polishing, which was performed in a solution of perchloric acid.

Table 1 Chemical Composition of EN X155CrMoV12 Tool Steel, wt.%

C	Si	Mn	P	S	Cr	Mo	V	W	Fe
1.58	0.26	0.32	0.01	0.01	12	0.16	0.4	0.01	Balance

Table 2 Mechanical and Thermal Properties at Room Temperature, 20 °C

UTS, MPa	Hardness, HRC	Thermal Conductivity, Wm^{-1} C^{-1}
720	30	20

Table 3 EDM Conditions

Polarity	Intensity of Discharge	Time of Discharge	Voltage of Discharge	Type of Tool	Dielectric Liquid
Positive	5 A	6 μs	46 V	Graphite	Hydrocarbon

3.2 Fatigue Tests

Tests were performed to determine the fatigue limit (defined as the stress giving a life of 10^6 cycles or greater) for the two machined conditions. Tests were performed at a frequency of 10 Hz in three-point bending with notched specimens, having a stress concentration K_t value of 1.6 (Fig. 2). The evolution of fatigue damage was monitored by scanning electron microscopy (SEM) at the root of the notch.

4. Results

4.1 Surface Characteristics

4.1.1 Roughness. Following EDM, the surface roughness was found to be characterized by roughness parameters R_a = 10 μm and R_t = 100 μm. Milling generally shows a better surface quality; we found lower values of average roughness R_a = 5 μm and maximum roughness depth R_t = 21 μm, for the milled samples.

In spite of the importance of these quantitative parameters, these data are not enough for a complete description of the surface topography obtained by EDM and characterized by typical craters (Fig. 3), very unlike a milled surface topography characterized by regular striations (Fig. 4).

4.1.2 Metallurgical Transformations. Optical metallography was performed on the machined samples using cross sections of machined pieces. No transformation was observed for the milled samples; however, the samples prepared by EDM show a layered structure resulting from the heat input during the machining process (Fig. 5). There are three discernible layers:

- A "white layer" near the surface, with a dendritic structure, resulting from re-solidification of metal melted during the electric discharge;
- A quenched layer with a martensitic structure just below the white layer; and
- A transition zone between the quenched layer and the base material.

Qualitative analysis of the surface chemical composition was performed by energy-dispersive x-ray analysis in SEM. This

Table 4 Milling Conditions

Cutting Speed, Vc	Feed per Tooth, fz	Depth of Cut, ap	Lubrication	Machining Tool	Machining Mode
30 m/min	0.05 mm	0.2 mm	Soluble oil	High speed cutter Diameter = 4 mm Number of teeth Z = 6	Peripheral milling, opposite

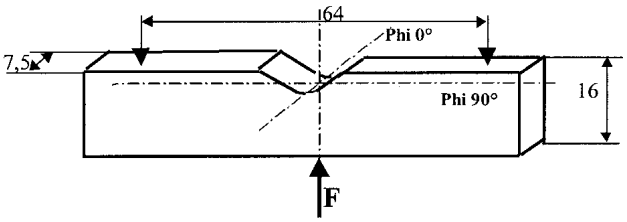

Fig. 2 Fatigue test specimen (dimensions in mm)

Table 5 XRD Conditions

Material	EN X155CrMoV12
Target	Cr
Wavelength $K_{\alpha 1}$, Å	2.2897
Filter	V
Diffraction plane *hkl*	211
Bragg Angle, °	156.3
Current	5 mA
Voltage	20 kV
Goniometer tilt	Psi
Beam section	Ø = 1,5 mm
Young's modulus, E, for steel	210 GPa
Poisson ratio, υ	0.33
Number of psi angles	13, from −36.3° to +39.2°
Number of phi angles	2, 0° and 90°

shows an increase in carbon content of the affected layers due to decomposition of the dielectric during the discharge (Fig. 6). No chemical modification was observed for the milling technique.

4.1.3 Hardness Modification. Microhardness measurements were made on transverse sections of machined samples. The EDM samples show a high degree of surface hardening: $HV_{0.1}$ = 1000 compared with $HV_{0.1}$ = 250 for the bulk material. This hardening is due to the near-surface phase transformations and the elevation of carbon content. The hardened layer has a depth of approximately 150 μm (Fig. 7).

The milled samples also show some hardening, but over a reduced depth of 100 μm, and with a maximum hardness of $HV_{0.1}$ = 450 (Fig. 8).

The modification to the near-surface layers can also be observed from the width of the XRD peaks (defined here as the width of the diffraction peak, in degrees, at 40% of the total peak height), as shown in Fig. 7 and 8. Broadening of the peaks occurs near the surface and can be attributed to an increase in dislocation density and lattice microstrain associated with the higher carbon content and phase transformations that occurred. The profiles of microhardness and peak broadening are similar, and they occur over the same depths beneath the surface.

4.1.4 Residual Stress. XRD residual stress measurement shows that, for the material machined by EDM, there is a tensile stress generated near the surface. The peak in the tensile stress lies about 50 μm below the surface, with a value of 750 MPa (Fig. 9).

For the milled material, the residual stresses are compressive at the surface. In this case, there is a difference in stress between the directions parallel and perpendicular to the motion of the milling tool. The direction parallel to the cutting motion shows a more compressive residual stress: approximately −300 MPa as compared with approximately −200 MPa (Fig. 10). The maximum residual stress is at the surface and reduces with depth.

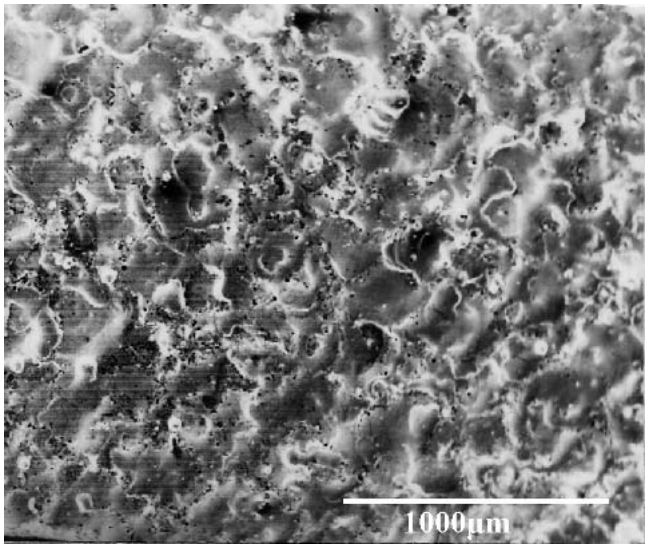

Fig. 3 Surface texture after EDM

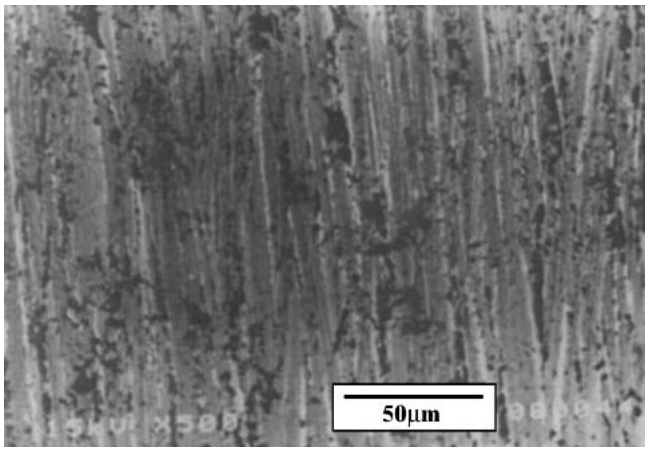

Fig. 4 Surface texture after milling

4.1.5 Surface Cracking. SEM observation of the EDM machined surfaces shows a network of microcracks (Fig. 11). About 8% of these have a depth greater than the white layer at the surface (Fig. 12). The presence of these cracks may also explain the reduction of residual stress at the surface.

4.2 Fatigue Behavior

4.2.1 Fatigue Limits. Results of fatigue tests, for samples prepared using EDM and by milling, are shown on an S-N plot in Fig. 13. The EDM samples show poorer fatigue properties over the entire range of applied stresses, and in the low cycle fatigue (LCF) and high cycle fatigue (HCF) regimes. The difference in behavior is particularly remarkable at lower stress amplitudes. It results in an endurance limit (at 10^6 cycles) of 165 ± 25

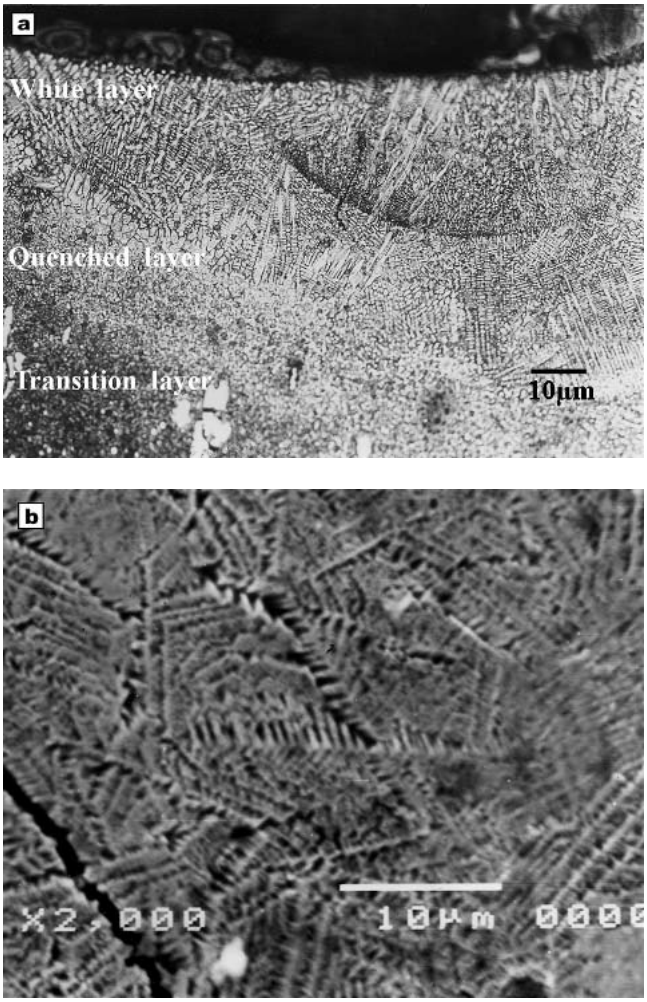

Fig. 5 Structure of near-surface layers affected by the EDM process: **(a)** gradient of structure in heat affected layers, **(b)** dendritic structure of surface melted steel

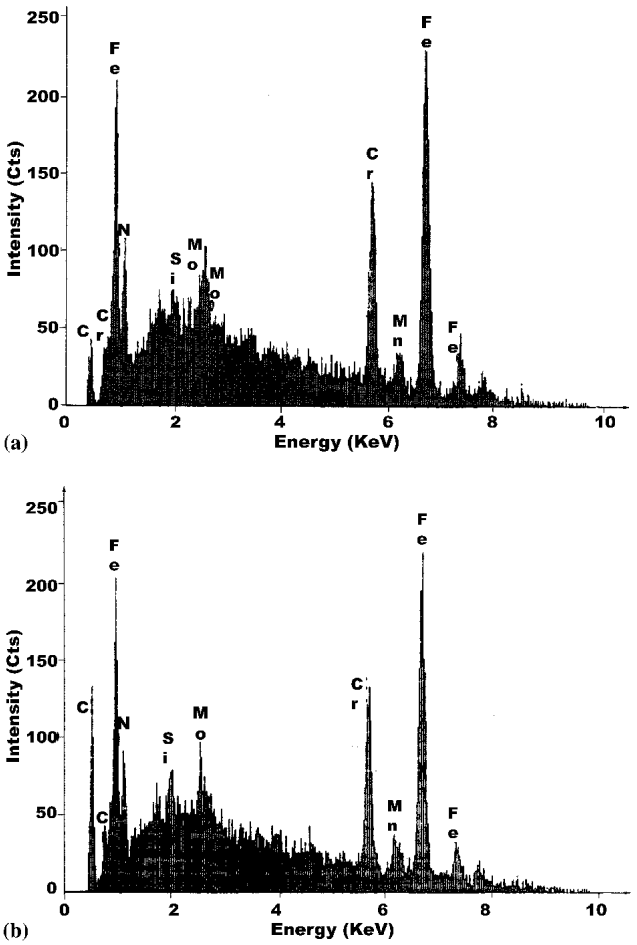

Fig. 6 Increase of carbon content with EDM (spectrum obtained in the same conditions): **(a)** base metal, **(b)** EDM surface

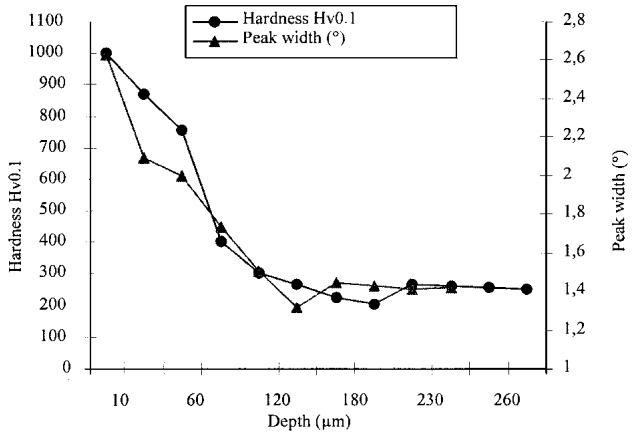

Fig. 7 Microhardness and x-ray peak broadening profiles after EDM

MPa for the EDM sample, which is significantly less than the corresponding value of 250 ± 12 MPa for the milled sample.

This reduction in the fatigue resistance can be attributed simply to the poorer quality of the surface following EDM.

4.2.2 Role of Machining Defects. SEM analysis of the surfaces and examination of regions near the notch root of the samples that were fatigue tested allows monitoring of the evolution of the network of cracks that was introduced by EDM. For these samples, it is difficult to identify an initiation stage of fatigue, due to the pre-existing distribution of thermal cracks (Fig. 11). This distribution of cracks changes appreciably whatever the level of applied stress; the cracks open and propagate readily to form a continuous network (Fig. 14 and 15). This leads to premature failure of the samples prepared by EDM, compared with those prepared by milling, which show better surface integrity and lower roughness.

4.2.3 Role of Residual Stress. To determine the role of the residual stresses on the fatigue process, it was deemed useful to follow the evolution of the residual stress during fatigue cycling at applied stress amplitudes equal to or greater than the endurance limit at 10^6 cycles. The results show, in both cases, a clear relaxation of the residual stress as a result of the cyclic plasticity.

The stress at the surface remains compressive for the milled samples (Fig. 16 and 17), while for the EDM samples, it changes from tensile to compressive when the applied load is

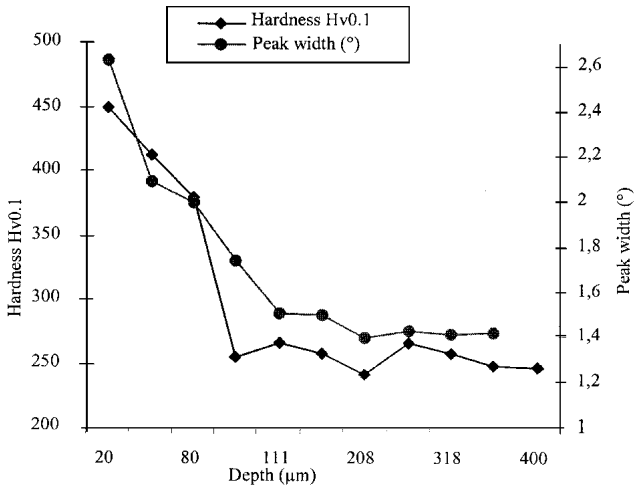

Fig. 8 Profiles of microhardness and x-ray peak broadening for the milled sample

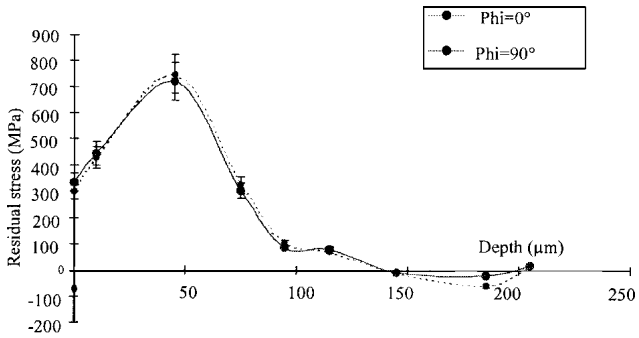

Fig. 9 Profile of residual stress after EDM

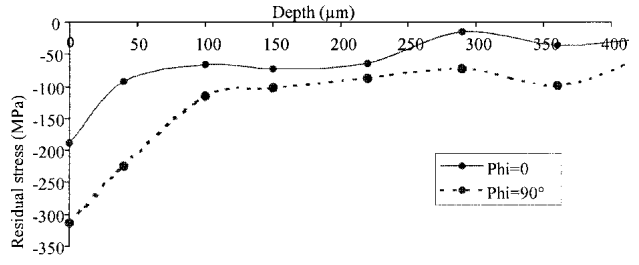

Fig. 10 Profile of residual stress after milling

high enough to cause plasticity from the root of the notch (Fig. 18). The plasticity can be observed by its effects on the widths of the XRD peaks (Fig. 19). A wider peak can indicate an increase in microstrain within the material, caused by the local strain fields around dislocations generated by plastic flow. Thus, there is noticeable broadening of the peak at around 30 μm below the surface and then reducing plasticity from that point onwards into the sample. The softening or annealing effect, which seems to have taken place at the surface, can be attributed to the partial disintegration of the brittle near-surface layers, caused by opening of the pre-existing cracks during cyclic loading, as seen by SEM examination (Fig. 14 and 15).

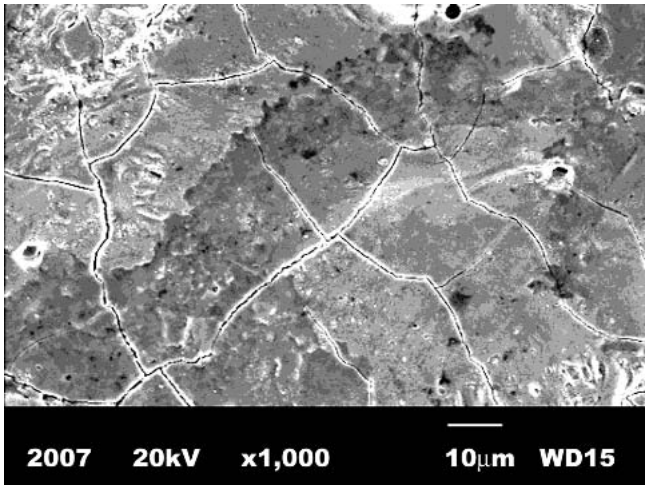

Fig. 11 Microcracking after EDM (from SEM surface observation)

5. Discussion

5.1 Surface Integrity

The term "surface integrity" was traditionally quantified solely in terms of observed surface cracking, but recent studies have attempted to broaden the concept by an examination of all the effects induced by a machining process.[19,20] The nature of these modifications, their exact values, and the depth of the affected layers depend on numerous interactions during the machining process. The main changes observed at the surface of EN X155CrMoV12 machined by EDM and milling are compared in Table 6. The results show a marked difference in surface integrity, arising from the different mechanisms that operate during the application of each process. In EDM, the metallurgical modifications in the near-surface layers are caused by the sparks that cause extreme local heating (up to 10 000 °C)[4,21] over a very short time (6 μs), and the subsequent cooling by the dielectric fluid and conduction into the bulk material. The thermal flux causes local evaporation of the metal at the surface, and the melting of a thin near-surface hollow of material. This leads to the formation of craters of varying sizes on the surface and is responsible for the uneven surface profile obtained using this method.

The macroscopic effect of the heating is to form transformed layers near the surface, from the melted layer, through a "quenched" layer, to a "tempered" layer, to the unaffected bulk material. The transformations depend on the precise thermal behavior of the material being machined and its ability to harden.[22,23] Under the conditions used in this study, no such thermal effects were observed with the use of milling. This is doubtless because the milling conditions used were not severe, and the steel was not heated sufficiently for phase transformation to occur.

For the milled samples, changes in surface hardness occur primarily due to work-hardening effects.[24,25] For the EDM samples, the hardness changes due to a combination of chemical and thermal effects.[4,6-8,21] This includes the effect of increased carbon content and changes introduced by the martensitic transformation in the quenched layer. The carbon

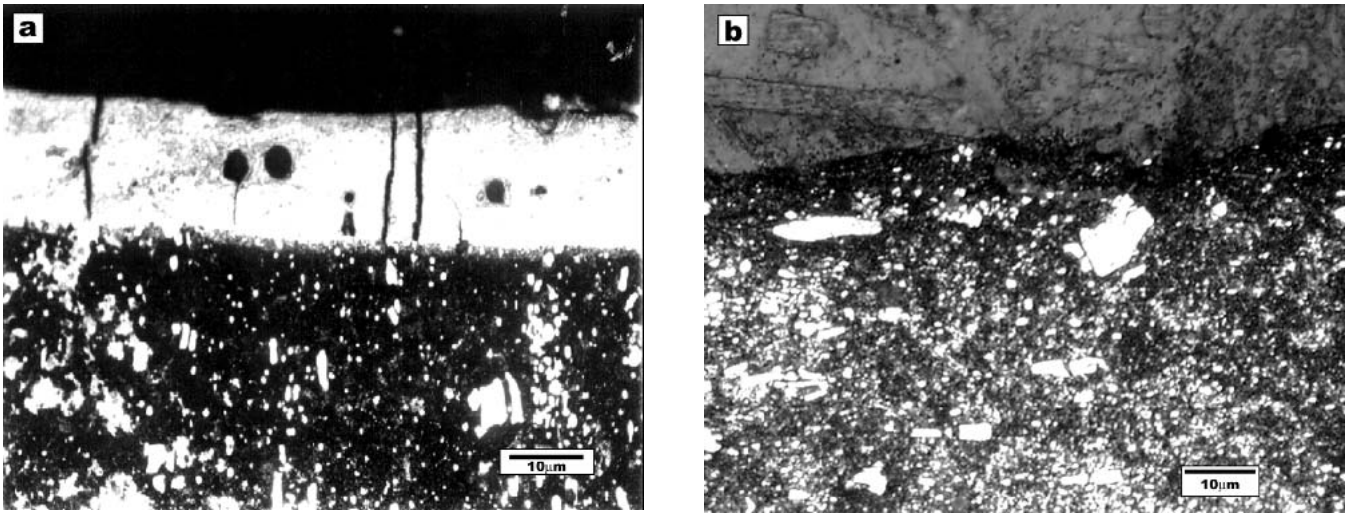

Fig. 12 **(a)** Cross section of an EDM sample, showing microcracking of the surface; **(b)** Cross section of a milled sample, no microcracking observed

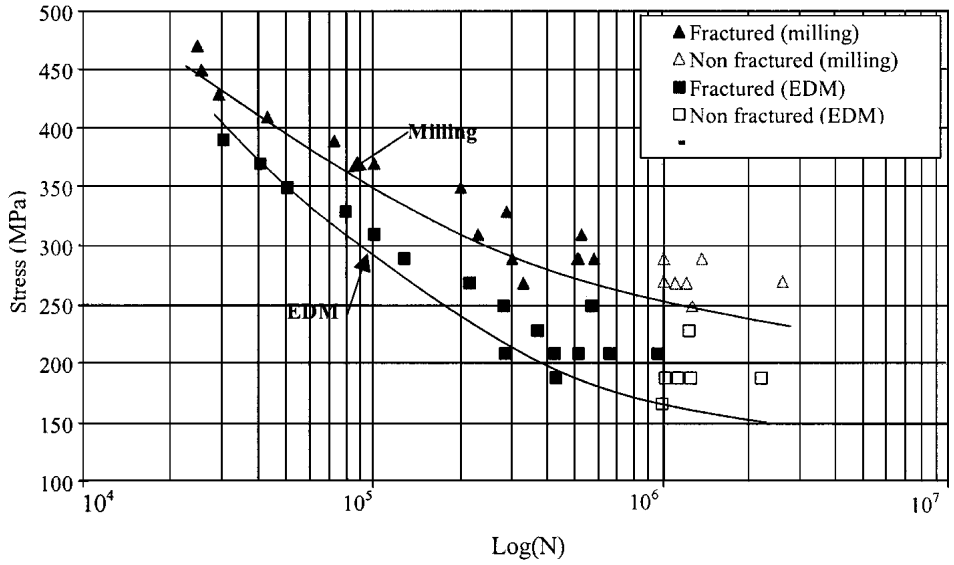

Fig. 13 Influence of the machining process on the fatigue life

diffusion results from the decomposition of the dielectric, as shown by the energy-dispersive x-ray results.

The strains generated by the thermal effects and phase transitions during EDM are responsible for the generation of the tensile residual stresses, which are generally observed in the literature for this process.[6,8,22,26,27] These stresses are partially relaxed at the surface, and it is likely that this is caused by the surface cracking associated with the use of EDM.[28,29] It is also possible that there is hydrogen diffusion into the surface layer following decomposition of the dielectric, which contributes to near-surface embrittlement.[23,30,31]

During milling, near-surface strains are generated by a combination of thermal and mechanical effects, and these lead to the generation of compressive surface stresses. The level of the stress generated depends critically on the properties of the material being machined and the machining conditions.[24,32]

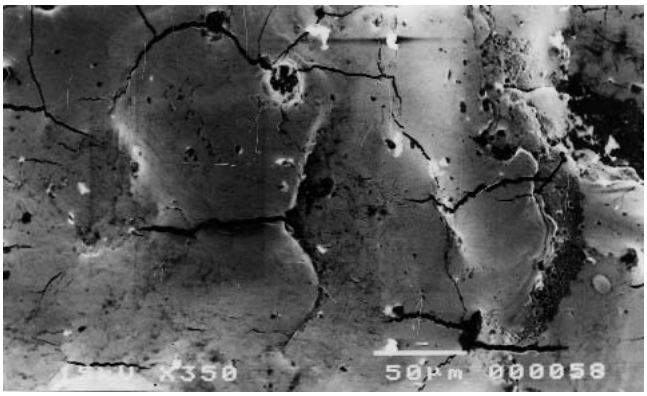

Fig. 14 Growth of microcracks on the EDM surface after 10^6 cycles at 166 MPa

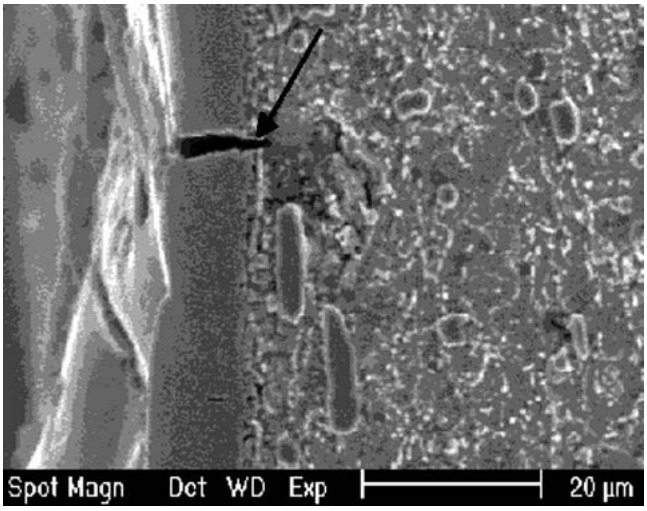

Fig. 15 Growth of microcracks from the EDM surface, from the white layer to the base metal, after 10^6 fatigue cycles at 166 MPa

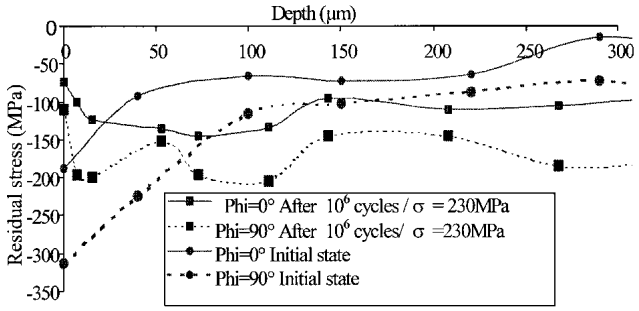

Fig. 16 Evolution of residual stress after fatigue test for milled specimens

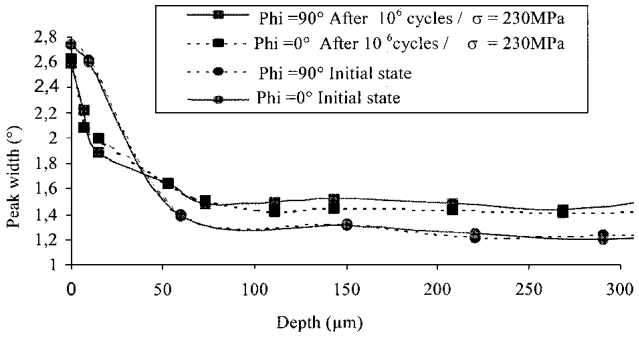

Fig. 17 Evolution of x-ray peak broadening after fatigue test for milled specimens

5.2 Fatigue Behavior of the Machined Surfaces

The results of this study confirm the importance of the relationship between surface integrity and the fatigue resistance of a component after machining. Here we characterized fatigue resistance by the endurance limit at 10^6 cycles.

The tensile residual stress distribution and the surface cracking are the two main parameters that explain the poorer fatigue resistance of the EDM workpieces. The milled samples have a

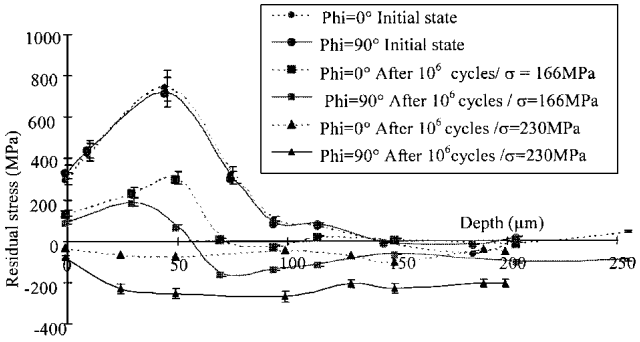

Fig. 18 Evolution of residual stress after fatigue testing for the EDM specimens

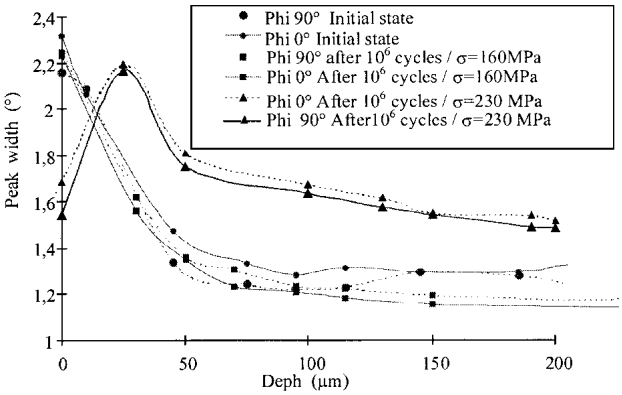

Fig. 19 Evolution of x-ray peak broadening after fatigue testing for the EDM specimens

better surface integrity, in terms of no surface cracking and a compressive residual stress state, which is known to improve fatigue life.[32,33] For low cycle fatigue, EDM and milled surfaces have closer fatigue behavior due to the residual stress relaxation resulting from significant cycling strain hardening in this cycle range; the fatigue crack propagation in bulk material is found to be the main factor controlling the fatigue life. This is because the hardening embrittlement of affected layers induced by both processes was almost identical. However, the milled surface without cracks exhibits higher fatigue limits. For high cycle fatigue behavior, which is generally initiation controlled, the presence of a residual stress can have a large effect on the measured life. A poor surface finish will always lead to earlier generation of fatigue cracking.

This result is compared with results from other thermal[18] and mechanical processes[6,7,16,17] in Table 7. From this we can conclude that conventional machining processes lead to better surface integrity and better surface quality regarding fatigue resistance. In this particular study, we note a decrease of about 35% in the endurance limit (at 10^6 cycles) for samples subjected to an EDM treatment rather than a milling treatment.

6. Conclusions

Thermal cycles involved in the material removal process in EDM lead to microstructural transformations, resulting, in the case of the EN X155CrMoV12 tool steel, in the creation of a

Table 6 Near-Surface Modifications Resulting From Machining, in Finishing Conditions, by EDM and Milling

Machining Mode	Roughness, µm	Metallurgical Transformations	Thickness of Hardened Layer, µm	Surface Hardness (a), $HV_{0.1}$	Residual Stresses, MPa	Surface Defects
EDM	$R_a = 10$ $R_t = 100$	Structure with three layers and carbon enrichment	150	1000	$\sigma_{surface}$ σ_{max} $\sigma_{\phi=0} = +350$ $\sigma_{\phi=0} = +750$ $\sigma_{\phi=90} = +350$ $\sigma_{\phi=90} = +750$	Thermal cracks
Opposite milling	$R_a = 5$ $R_t = 21$	No apparent transformations	100	450	$\sigma_{\phi=0} = -300$ $\sigma_{\phi=0} = -300$ $\sigma_{\phi=90} = -200$ $\sigma_{\phi=90} = -200$	No apparent defects

(a) Bulk hardness = $250HV_{0,1}$

Table 7 Influence of EDM on the Fatigue Behavior and Comparison to Other Machining Processes

Steel Type	Fatigue Test Conditions: Type	Fatigue Test Conditions: Run-out Cycles	Surface Residual Stress σ_R, MPa	Fatigue Life Decrease Compared to Reference Process	Reference Process	Reference
X210Cr12	Alternating bending	10^7	+800	50%	Turning	[6]
40NCD16	Rotating bending	10^6	+350	50%	Drilling	[7]
S45C 0.45% C steel	Rotating bending	10^7		10-60%	Grinding	[16]
D20 90% WC, 7% Co, 3% TiTac	Rotating bending	10^7		55-66%	Mechanical polishing	[17]
Carbon steel	Alternating bending	10^7	+220	13%	Laser cutting	[18]
EN X155CrMoV12	3-point bending	10^6	+350	35%	Milling	This study

structure with three different layers and a tensile residual stress at near surface. They also lead to near-surface hardening and microcracks.

This poor surface integrity state noticeably decreases the integrity of the surface, and the fatigue resistance in particular, compared with surfaces finished by milling, which do not show significant metallurgical transformation or microcracks.

The surfaces prepared by EDM show a tensile residual stress at the surface; milled surfaces show a near-surface compressive residual stress, which is favorable for fatigue crack resistance.

References

1. H. Hocheng, W.T. Lei, and H.S. Hsu: "Preliminary Study of Material Removal in Electrical-Discharge Machining," *J. Mater. Process. Technol.,* 1997, *63,* pp. 813-18.
2. AGIE : "Electroérosion coup de projecteur sur de la haute production," *Machine Production,* 1993, *6*, pp. 49-52 (in French).
3. B.H. Yan, F.Y. Huang, H.M. Chow, and J.Y. Tsai: "Micro-Hole Machining of Carbide by Electric Discharge Machining," *J. Mater. Process. Technol.,* 1999, *87*(1-3), pp. 139-45.
4. E. Bud Guitrau: *The EDM Handbook,* Hanser Gardner Publications, Cincinnati, OH, 1997.
5. H Gripenberg: "Effects of EDM on Surface Residual Stresses in a TMCP Steel" in *Proc. of The Sixth International Conference on Residual Stresses (ICRS-6),* G.A. Webster, chr., IOM Communications, London, UK, 2000, pp. 1004-11.
6. J. Grosch: "Influence de l'usinage par électroérosion sur la microstructure superficielle de différents aciers," *HTM 44,* 1991, pp. 290-95 (in French).
7. B. Hosari: "Etude de l'enlèvement de matière par électroérosion assisté par ultrasons," Ph.D. Thesis, ENSAM, Paris, France, 1988 (in French).
8. A.G. Mamalis, G.C. Vosniakos, and N.M. Vaxevanidis: "On the Surface Integrity of Mechanically and Thermally Worked Metal Plates," *Advanced Technology of Plasticity, 1*, 1987, pp. 407-14.
9. AGIE: "Controlling EDM Surface Integrity," *American Machinist and Automated Manufacturing, 11*, 1987, pp. 81-83.
10. H.P. Lieurade: "Effet des contraintes résiduelles sur le comportement à la fatigue des pièces et des structures industrielles," *Traitement thermique,* PYC édition, Paris, France, 1988, pp. 15-28 (in French).
11. A. Brand and J.F. Flavenot: "Données technologiques sur la fatigue," Publications CETIM, France, 1993 (in French).
12. A. Pailleux and F. Convert: "Qualité des outillages de presse usinés par électroérosion," CETIM informations, 1980, *64,* pp. 44-51 (in French).
13. J. Bergstrom and G. Fredriksson: "Fatigue of Cold Work Tool Steel," *Bulletin du cercle d'étude des métaux,* France, 1998, *16*(17) pp. 4.1-4.10 (in English).
14. P. Miller, U.A. Guha, and B. Wellman: "Effects of Electrical Discharge Machining on the Surface Characteristics of Mold Materials," *J. Injection Molding Technol.,* 1998, *2*(3), pp.128-36.
15. O.A. Abu Zeid: "On the Effect of Electrodischarge Machining Parameters on the Fatigue Life of AISI D6 Tool Steel," *J. Mater. Process. Technol.,* 1997, *68*(1), pp. 27-32.
16. T. Tsutsui and T. Tamura: "Effect of the Electro-Discharge Machined Surface of the Mechanical Properties—On the Fatigue Strength of Carbon Steel," *Bull. Jpn. Soc. Precis. Eng.,* 1984, *18*(45), pp. 341-42.
17. T. Tsutsui and T. Tamura: "Effect of the Electro-Discharge Machined Surface of the Mechanical Properties—On the Fatigue Strength of Cemented Carbide," *Bull. Jpn. Soc. Precis. Eng.,* 1987, *21*(1), pp. 70-71.
18. K. Iida and K. Tosha: "Fatigue Strength of Shot Peened Specimen Formed by Laser Cutting and Wire EDM," *Bull. Jpn. Soc. Precis. Eng.,* 1988, *22*(3), pp.195-89.
19. A.M. Abrao and D.K. Aspinwall: "The Surface Integrity of Turned and Ground Hardened Bearing Steel," *Wear,* 1996, *196*(1-2), pp. 279-84.
20. Y.K. Chou and C.J. Evans: "White Layers and Thermal Modeling of Hard Turned Surfaces," *Int. J. Machine Tools Manuf.,* 1999, *39*(12), pp. 1863-81.
21. Atelier Des Charmilles: "Introduction à l'usinage par électroérosion," *Techniques Industrielles,* 1983, *144,* pp. 51-77 (in French).
22. J.C. Rebelo, A. Morao Dias, D. Kremer, and J.L. Lebrun: "Role of

EDM Machining Parameters on Surface Integrity of Martensitic Steels for Mould Industry" in *Proc. of The Fifth International Conference on Residual Stresses (ICRS-5),* T. Ericson, M. Odéon, and A. Andersson, ed., Institute of Technology Linköping Universitat, Linköping, Sweden, *1,* pp. 163-67.

23. F. Ghanem, H. Sidhom, and C. Braham: "An Engineering Approach to the Residual Stresses Due to Electric-Discharge Machining Process" in *Proc. of The Fifth International Conference on Residual Stresses (ICRS-5),* T. Ericson, M. Odéon, and A. Andersson, ed., Institute of Technology Linköping Universitat, Linköping, Sweden, *1,* pp. 157-62.
24. W. Bouzid Saï and N. Ben Salah: "Influence of Machining by Finishing Milling on Surface Characteristics," *Int. J. Machine Tools Manuf.,* 2001, *41,* pp. 443-50.
25. M. Elbestawi and L. Chen: "High-Speed Milling of Dies and Models in Their Hardened State," *CIRP Ann.*, 1997, *46*(1), pp. 57-62.
26. P. Noaker: "EDMachining Tool Steel," *Tooling and Production,* 1988, Feb, pp. 63-65.
27. J. Prata Pina, M. Dias,, and J.L. Lebrun: "Study of Residual Stresses and Cold Working Generated by Machining of AISI H13 Steel" *Proc. of Second International Conference on Residual Stresses (ICRS2),* G. Beck, S. Denis, and A. Simon, ed., Elsevier Applied Science, 1989, pp. 690-95.
28. L. Lee and L.C. Lim: "Quantification of Surface Damage of Tool Steels After EDM," *Int . J. Mach. Tools Manuf.,* 1988, *28,* pp. 359-72.
29. C.J. Heuvelman: "Summary Report on the CIRP Cooperative Research on Spark-Erosion Machining of Cemented Carbides," *Ann. CIRP,* 1980, *29*(2), pp. 541-44.
30. C.K. Chow, G.R. Brady, V. F. Urbanic, and C.E. Coleman: "Hydrogen Ingress Through EDM Surfaces of Zr-2.5Nb Pressure Tube Material," *J. Nucl. Mater.,* 1998, *257,* pp. 35-43.
31. S.L. Chen, B.H. Yan, and F.Y. Huang: "Influence of Kerosene and Distilled Water as Dielectrics on the Electric Discharge Machining Characteristics of Ti-6A1-4V," *J. Mater. Process. Technol., 87,* 1999, pp. 107-11.
32. S. Brunet: "Influence des contraintes résiduelles induites par usinage sur la tenue en fatigue des matériaux métalliques aéronautiques," Ph.D. Thesis, ENSAM, Paris, France, 1991 (in French).
33. A. Couturier and I. Peyrac: "Machining or Shot Peening Residual Stress Effects on the Fatigue of Aluminium Matrix," *Technol. Transfer Ser., 2*, 1997, pp. 287-97.